

3D Metallo-Dielectric Photonic Crystals with Strong Capacitive Coupling between Metallic Islands

D. F. Sievenpiper and E. Yablonovitch

Electrical Engineering Department, University of California, Los Angeles, California 90095-1594

J. N. Winn, S. Fan, P. R. Villeneuve, and J. D. Joannopoulos

Department of Physics, Massachusetts Institute of Technology, Cambridge, Massachusetts 02139

(Received 10 November 1997)

We introduce a new type of metallo-dielectric photonic band gap structure (PBG), intentionally incorporating very strong capacitive interactions between the periodic metallic islands. The band gaps become huge, with the lower band edge frequency being pushed down by the capacitive interaction between metallic islands, while the upper band edge frequency continues to depend primarily on the lattice constant, as in normal PBG's. With this new type of photonic crystal, the spatial periodicity can be much smaller than the corresponding electromagnetic wavelength, allowing PBG structures to play a role at radio frequencies. [S0031-9007(98)05629-4]

PACS numbers: 42.70.Qs, 41.20.Jb, 78.70.Gq, 84.40.-x

Photonic band gap structures (PBG's) are artificial dielectric structures in which periodicity gives rise to stop bands for electromagnetic waves [1,2]. In the past few years, a new class of PBG's has emerged in which metallic islands are incorporated into the 3D dielectric lattices [3-8]. If these metallic components are isolated from one another, then the band structure resembles that of conventional dielectric/air photonic crystals, with the electromagnetic fields tending to concentrate within the dielectric phase. However, as the metal islands are made larger, they can almost touch, producing strong capacitive interaction between them, and changing the nature of the band structure. Furthermore, as the capacitance gets higher, the band gaps increase, becoming even wider than the already large band gaps of ordinary metallo-dielectric PBG's.

Under increased capacitive coupling in our structures, we find that the upper, or "conduction" band edge frequency remains fairly constant, but that the lower, or "valence" band edge is pushed down to very low frequencies, creating a huge band gap. The effect of closely spaced capacitive metallic plates is a medium with a very high effective dielectric constant, accounting for the very wide band gaps. This makes possible low frequency PBG structures of spatial periodicity much finer than the corresponding free-space electromagnetic wavelength. We can anticipate that these PBG structures will be small enough and light enough to be useful at radio frequencies.

As is the case for dielectric PBGs, metallo-dielectric structures with the topology (connectivity) of the diamond crystal tend to have large band gaps [9]. Our structure can be regarded as an intermediate case between two opposing limits of metallo-dielectric diamond structures which have been studied previously: a three-dimensional conducting wire mesh configured in a diamond lattice [3], and at the other extreme, a diamond lattice of unconnected, metal spheres [4].

If the wire mesh structure forms a continuous network, long waves cannot penetrate the conducting mesh, and the band gap extends to zero frequency. The cutoff, or conduction band frequency is a function of the lattice constant of the crystal. If defects are added, by inserting capacitors into some of the wires, individual electromagnetic modes are pulled down into the band gap. As more capacitors are added [3], breaking the continuous conducting paths, these states merge into a valence band. The frequency of the valence band is determined by the capacitance and inductance of the wires.

At the opposite limit is a diamond lattice of unconnected metal spheres. As the spheres get closer together, the valence band edge is pushed lower in frequency, and the gap gets wider. If the spheres get close enough to touch, forming a continuous network of metal, the gap extends to zero frequency, as in the connected wire mesh described above. When the spheres are very close, but not quite touching, the gap can be extremely wide. In this limit, the spaces between the spheres resemble the capacitors inserted in the wire mesh photonic crystal.

In both cases, the valence band edge frequency is determined by the capacitance between the metal islands, while the conduction band edge frequency is determined mainly by the lattice constant. We believe that the detailed shape of the metallic elements does not matter, only the topology of the capacitive connections between them, and that any capacitive metal structure with diamond connectivity should behave in a similar manner.

This qualitative behavior is illustrated in Fig. 1, which shows the conduction band edge frequency being determined by the spatial periodicity, $\omega_v \approx \pi c/na$, and the valence band edge frequency being controlled by the capacitance, $\omega_v \approx 1/\sqrt{LC}$, where a is the spatial periodicity, c/n is the phase velocity of light in the dielectric, and the capacitance C and inductance L are determined by

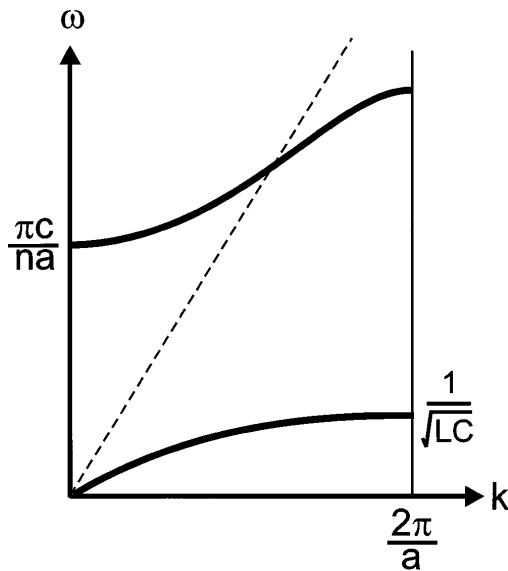


FIG. 1. A schematic illustration of the conduction and valence band edge frequencies being separately controlled by the spatial periodicity a and capacitive coupling C , respectively. $\omega_v \approx \pi c/na$, and $\omega_c \approx 1/\sqrt{LC}$. The dashed line has a slope of c/n .

geometrical aspect ratios. In our case, L scales according to the length of the wires or metallic elements, but L can also be increased by making the wires unusually narrow [5].

We chose printed circuit board technology for fabricating our capacitively coupled PBG structures, which allows large capacitance, and features sizes that are appropriate to microwave wavelengths. The circuit boards are stacked and bonded together to form 3D, periodic structures, and the combination of vertical metal vias and horizontal wiring allows many different topologies to be implemented. High capacitance is achieved by stacking the boards very close together, with facing metallic elements separated by thin dielectric layers.

In our geometry, the circuit boards represent the $\langle 001 \rangle$ planes of the diamond crystal. The substrate is Rogers Duroid 5880, a commercial microwave circuit board material [10] with a dielectric constant of $n^2 = \epsilon = 2.2$. As shown in Fig. 2, the tetrahedral atomic bond arrangement of diamond is mimicked by two $0.66 \text{ mm} \times 1.98 \text{ mm}$ rectangular metal patches, at right angles, connected at their centers by a metal plated hole. Capacitive interconnections are made by stacking the circuit boards so that the two ends of each rectangular patch overlap with the ends of two neighboring patches on each adjacent circuit board, separated by a $25 \mu\text{m}$ thick layer of polyimide ($\epsilon = 4$). The full stack is then bonded together with phenolic butyral adhesive.

Thus, each tetrahedral metal island is connected to each of its four neighbors by a metal/polyimide/metal capacitor, completing the diamond connectivity. As in $\langle 001 \rangle$ diamond orientation, there is an $a/2\sqrt{2}$ shift for each successive layer, and a 90° rotation, so that four

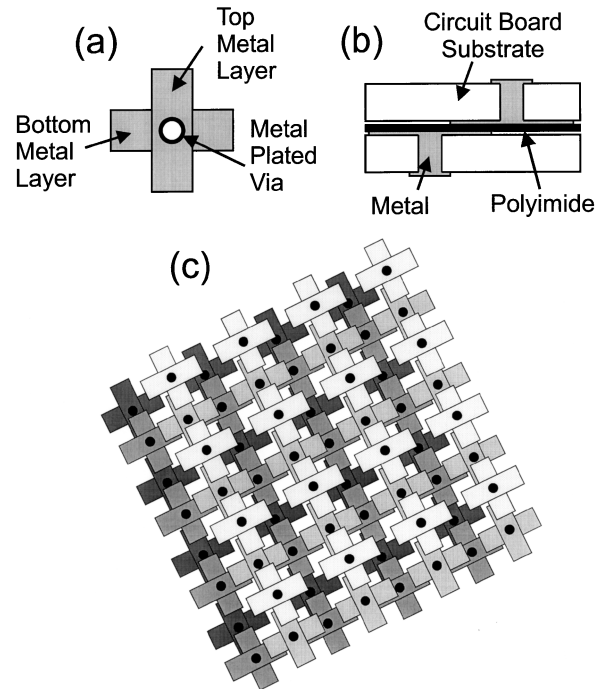


FIG. 2. (a) The tetrahedral bond geometry of diamond is created by two rectangular metal patches, on opposite sides of a circuit board, facing each other at right angles and connected center to center by a metal plated cylinder. (b) The circuit boards are $775 \mu\text{m}$ thick, and the metal layers on either side are $80 \mu\text{m}$ thick. Capacitors are formed between metal elements on adjacent boards using a $25 \mu\text{m}$ thick polyimide insulator. (c) Four layers form one period of the diamond lattice in a top view.

layers form one period. Our experimental structure is 13 layers thick, or 3.25 face-centered cubic unit cells. The edges of the structure are $\langle 110 \rangle$ planes, and each edge is $20/\sqrt{2}$ unit cells long. The unit cube length is $a = 3.73 \text{ mm}$, and the capacitance in the “valence bonds” is $0.54 \text{ pF} \pm 8.5\%$.

We began our experimental study with plane wave transmission measurements. Mode frequencies were identified with step function changes in the transmission spectrum, which the internal wave vectors were determined by wave-vector matching at the crystal surface. Because of the planar geometry and finite size of the experimental sample, only a limited region of k space can be measured. The data from these experiments are plotted as solid points in Fig. 3, for comparison to the calculated band structure. A band gap was found covering a range of 12–30 GHz, with as much as 35 dB of rejection relative to the band edge transmission.

At normal incidence, symmetry prevented coupling to the lowest conduction band, making the band gap appear to extend up to 40 GHz. The modes at the bottom of this band have the electric field oriented primarily along the Z direction, so they are visible only with TM polarized, off-axis waves, which have electric field components normal to the surface.

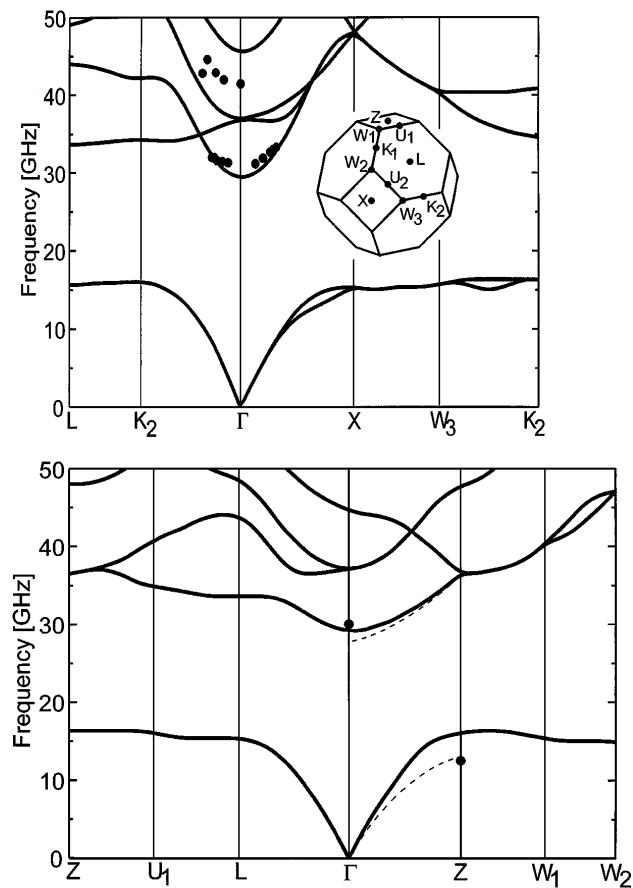


FIG. 3. Calculated band structure for capacitively loaded, metallo-dielectric photonic crystal. Solid lines are for capacitor plate spacing 3 times wider than in the experimental structure. Dashed lines are for calculations with the correct plate spacing. Filled dots are experimental data points. The band gap is clearly omnidirectional.

We verify that the band gap is omnidirectional by using monopole antennas, consisting of a short metal pin extending from the center conductor of a coaxial cable. By acting as a point source, the monopoles sample all wave vectors in k space, including those that are inaccessible to external plane waves, and thus serve as an effective tool for determining whether the band gap is complete and omnidirectional. A representative plot of transmission vs frequency is shown in Fig. 4. In this case, the probes were positioned on either face of the photonic crystal, with the pins directed towards each other, permitting coupling to the Z polarized modes that lie between 30–40 GHz. The measured gap spans 12–30 GHz, in agreement with the plane wave measurements.

We have also computed the band structure of this new type of metallo-dielectric photonic crystal, and the theoretical results confirm that the band gap is indeed omnidirectional. The band structure calculations are based on a finite-difference time-domain method, in which the electromagnetic fields are discretized on a rectangular grid, and Maxwell's equations are approximated by difference equations on the grid. For each wave vector, we used

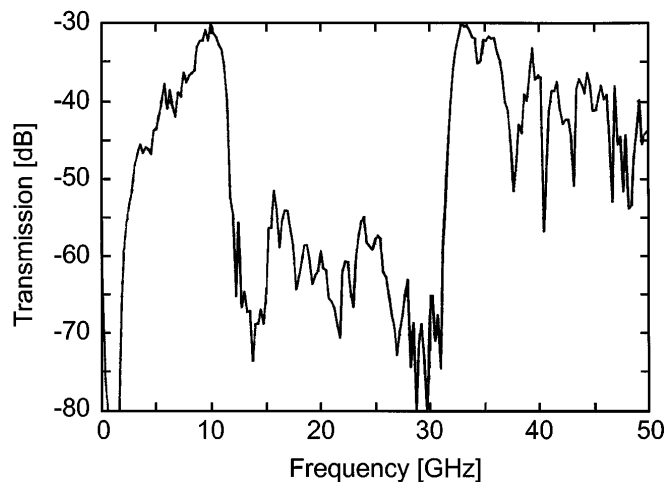


FIG. 4. Transmission vs frequency for monopole probes directed into the surface of the crystal. The monopole probes sample all wave vectors, and verify that the band gap is omnidirectional over a range of 12–30 GHz.

a Bloch boundary condition, $E(r + R) = e^{ikR}E(r)$, and excited the fields with current sources whose location and phases are compatible with this condition. Calculations were performed using a $68 \times 68 \times 104$ grid, for a duration long enough to distinguish two modes which differ by 0.2 GHz. The electromagnetic fields were then decomposed by Fourier transformation to obtain the eigenmode frequencies for each wave vector. For more details on this method see [4]. The results of the calculations are plotted in Fig. 3, with experimental data points superimposed for comparison. The most significant feature of the band structure calculations is the wide, omnidirectional gap between the second and third bands.

Most of the computations involved a structure in which the spacing between capacitor plates was 3 times wider than in the experimental structure. This allowed a coarser grid to be used, permitting the complete band structure to be calculated with limited computer memory and processor time. This change causes an increase in the lower band edge, which depends strongly on the capacitance, but does not affect the overall shape of the band structure. To verify this, we recomputed the bands from $k = \Gamma$ to Z for structures with the correct plate spacing. These calculations are plotted as dashed lines in Fig. 3. The computed band gap spanned 13–28 GHz, in good agreement with experiments. Other discrepancies, including the disagreement with experiments of the higher bands, may be the result of field discretization and incorrect spacing in the computations and experimental uncertainties. The main point is that the calculations confirm the critical features of the experiments: the frequencies of the band edges, and the omnidirectional nature of the band gap.

In dielectric photonic crystals, the valence band electric fields reside primarily in the high dielectric constant material, while the conduction band electric fields inhabit the low dielectric constant material. The maximum

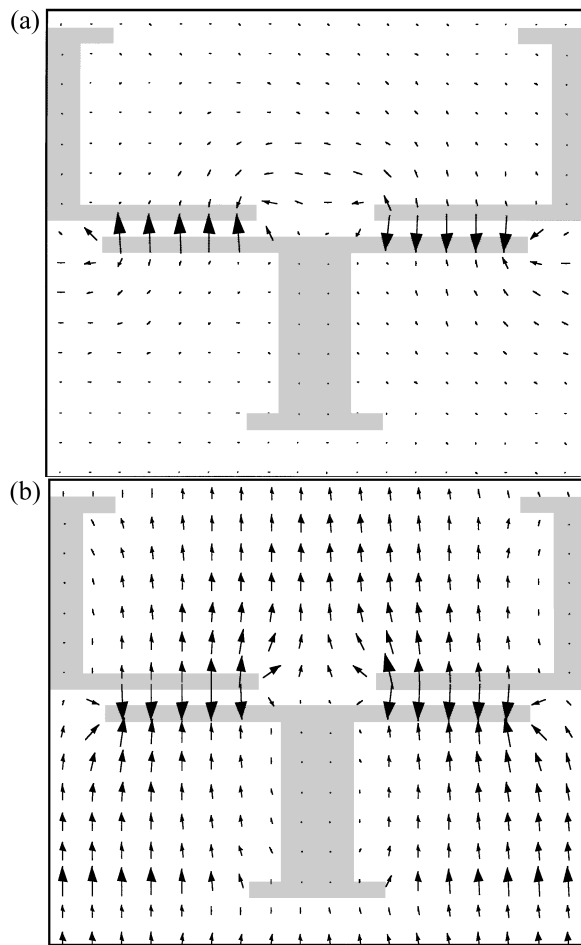


FIG. 5. (a) Calculated electric field plots for a state at the edge of the valence band at Z, shown in a $\langle 110 \rangle$ cross section. The electric field is primarily concentrated in the regions between the capacitor plates. (b) A state at the bottom of the conduction band near Γ . The electric field is primarily Z polarized and is concentrated in the large areas between the metal regions.

achievable band gap is determined by the dielectric contrast between the two media. In metallo-dielectric photonic crystals, the metal elements exclude electric fields, producing a rather different spatial mode distribution. In the valence band, the electric field is concentrated in the narrow region between the capacitor plates, as shown in Fig. 5(a). Here, the structure resembles a low pass electric filter. The frequency of the valence band edge is given by $\omega_v \approx 1/\sqrt{LC}$, where C is the capacitance, and L is the inductance of the metal elements, which depends mainly on the spatial period. Therefore, the valence band edge frequency can be independently controlled by varying the capacitance between the metal islands.

The conduction band electric field fills the large dielectric tunnels between the metallic elements, as shown in Fig. 5(b). Generally, one half-wavelength fits in these regions, occupying the Duroid circuit board material. Thus, the conduction band edge frequency is given by $\omega_v \approx \pi c/na$.

Because of the planar (not tetrahedral) arrangement of the metals, our structure has a smaller symmetry group than a true diamond lattice. The Z direction differs from the X and Y directions. What would be three degenerate modes in the conduction band are split into a single, nondegenerate mode (polarized primarily in the Z direction) and a pair of modes which are related by a 90° rotation in the XY plane. These last modes occupy the $\langle 110 \rangle$ channeling tunnels in the XY plane, whose X/Z geometrical aspect ratio $\approx 4/3$, accounting for the frequency difference between Z vs X-Y polarized waves.

The important properties of capacitively loaded metallo-dielectric photonic crystals can be summarized as follows: (1) The band gap is wider than what was previously possible with dielectric photonic crystals, or even what was practical with other structures involving metals. (2) The frequency of the valence and conduction bands can be tuned independently by varying two different parameters, the capacitance and the lattice constant. (3) The structure is easily designed and fabricated with printed circuit boards, a mature and readily available technology.

Most importantly, if the capacitive coupling is sufficient, then the spatial periodicity of these PBG structures can be much smaller than the valence band edge vacuum wavelength. This will allow the use of small and light-weight PBG structures at radio frequencies.

This work is supported by Army Research Office Grant No. DAAH04-96-1-0389, and Hughes Research Laboratory Subcontract No. S1-602680-1. J.N.W. thanks the Fannie & John Hertz Foundation for financial support. The authors thank Bernard Soffer for helpful discussions and comments on the manuscript.

- [1] J.D. Joannopoulos, R.D. Meade, and J.N. Winn, *Photonic Crystals* (Princeton University, Princeton, 1995).
- [2] See, for example, the articles in the special issue of *J. Opt. Soc. Am. B* **10** (February, 1993).
- [3] D.F. Sievenpiper, M.E. Sickmiller, and E. Yablonovitch, *Phys. Rev. Lett.* **76**, 2480 (1996).
- [4] S. Fan, P.R. Villeneuve, and J.D. Joannopoulos, *Phys. Rev. B* **54**, 11 245 (1996).
- [5] J.B. Pendry, A.J. Holden, W.J. Stewart, and I. Youngs, *Phys. Rev. Lett.* **76**, 4773 (1996).
- [6] E.R. Brown and O.B. McMahon, *Appl. Phys. Lett.* **67**, 2138 (1995).
- [7] K.A. McIntosh, L.J. Mahoney, K.M. Molvar, O.B. McMahon, S. Verghese, M. Rothschild, and E.R. Brown, *Appl. Phys. Lett.* **70**, 2937 (1997).
- [8] M.M. Sigalas, C.T. Chan, K.M. Ho, and C.M. Soukoulis, *Phys. Rev. B* **52**, 11 744 (1995).
- [9] C.T. Chan, K.M. Ho, and C.M. Soukoulis, *Europhys. Lett.* **16**, 563 (1991).
- [10] Available from Rogers Corporation, 100 S. Roosevelt Ave., Chandler, AZ 85226; <http://www.rogers-corp.com/>